CeO$_2$ BUFFER LAYERS ON R-PLANE Al$_2$O$_3$[*]

Š. Chromik, M. Španková, I. Vávra, Š. Gaži
*Institute of Electrical Engineering, Slovak Academy of Sciences, Dúbravská cesta 9,
842 39 Bratislava, Slovak Republic*

M. Cannaerts
*Laboratorium voor Vaste Stof-Fysika en Magnetisme, Katholieke Universiteit Leuven,
Celestijnenlaan 200 D, B-3001, Belgium*

L. Hellemans
*Department of Chemistry, Katholieke Universiteit Leuven, Celestijnenlaan 200 D, B-3001,
Belgium*

D. Machajdík, Š. Beňačka
*Institute of Electrical Engineering, Slovak Academy of Sciences, Dúbravská cesta 9,
842 39 Bratislava, Slovak Republic*

We present a summary of some published results concerning the preparation and study of the properties of CeO$_2$ buffer layers on R-plane Al$_2$O$_3$. Further, we discuss some of our results which concern to CeO$_2$ films prepared by electron gun-evaporation, by on-axis rf magnetron sputtering in mixture of Ar and O$_2$ and by off-axis rf diode sputtering in pure oxygen. As-deposited films show granular structure except for films prepared by electron gun-evaporation which already consist of rectangular blocks. Atomic Force Microscopy (AFM) reveals that the presence of even negligible (111) parasitic peak in X-ray diffraction spectrum of the as-deposited films strongly influences the rocking curve and surface morphology after post-deposition heat treatment in air. The post-annealings suppress (111) peak in X-ray spectrum, however, the rocking curves and AFM results differ depending on the method of preparation. Some rocking curves seem to be a superposition of a very narrow rocking curve (0.04°) with a broader one (0.5-1.4°). The origin of such behaviour is discussed.

1 Introduction

Cerium oxide (CeO$_2$) thin films are good buffer layers for the growth of superconducting YBa$_2$Cu$_3$O$_x$ (YBCO) and Tl-based thin films on sapphire substrates [1-10]. CeO$_2$ films prevent interdiffusion and provide good lattice matching to the superconducting films. In this paper we compare different deposition methods for the CeO$_2$ films. Structural properties and the surface morphology of the layers are also analyzed.

---

[*]Presented at the Workshop on Solid State Surfaces and Interfaces II, Bratislava, Slovakia, June 20 – 22, 2000.

2   Epitaxial film deposition

CeO_2 films can be grown on R-cut Al_2O_3 ($1\bar{1}02$) by a wide variety of deposition methods and can be optimized to have very smooth surface morphology. The most frequently used deposition techniques for the CeO_2 are pulsed laser deposition (PLD), sputtering, and evaporation.

The film deposition by PLD is carried out by irradiation of a single target by a focused laser beam (e.g. KrF, λ=248 nm, t=30 ns) [2, 3, 8]. The typical substrate temperature is in the range 700-750°C. Ceramic targets are ablated with an energy density Q=1 J/cm^2 in an oxygen atmosphere $\approx$ 20 Pa. Main advantages are high rate stoichiometric deposition and process flexibility. However PLD is limited to small areas (typically 1 cm^2) and the pulsed deposition has often impact on the morphology (droplets).

Sputter deposition is widely used for the successful preparation of the CeO_2 films [1, 6, 7, 9, 10]. The most serious problem at this deposition method is resputtering due to the presence of oxygen ions in plasma which bombard the substrate. The method to avoid this problem is to thermalize the energetic species by sputtering at very high pressure [1, 10] or by using "off-axis" [9] sputtering, where the substrate is positioned out of the high-energy particles flux which is directed mainly perpendicular to the target surface. We routinely use on-axis [10] and off-axis [9] rf sputtering from a single, pressed and sintered stoichiometric target. In case of on-axis sputtering the deposition of 60 nm thick CeO_2 film in a mixture of Ar and O_2 at ratio of 4:1 and the total pressure of 50 Pa was used. The growth rate was 1 nm/min. The rf power on the target and substrate temperature were 80 W and 750°C, respectively. Off-axis sputtering was used for the preparation of 15-100 nm thick films. They were grown at an rf power of 30 W and at substrate temperatures 640-800°C. A mixture of Ar and O_2 by volume 1:1 or pure O_2 at the total gas pressure of 8 Pa were used as sputtering gases. The growth rates were 0.5 nm/min in the gas mixture and 0.35 nm/min in pure O_2.

Electron beam evaporation of the CeO_2 is a simple method [4, 5] enabling to prepare large-area epitaxial layers. However CeO_2 can be reduced to nonstoichiometric CeO_x with $2 > x > 1.5$ using reduced oxygen partial pressure and higher temperatures during the deposition. CeO_x can be reoxidized easily in atmospheric oxygen to form stoichiometric CeO_2 [11]. In our case, we have prepared CeO_2 films by electron gun-evaporation of ceramic CeO_2 source at oxygen partial pressure 10^{-2} Pa and substrate temperature 850°C. The thickness of the films was in the range 50-150 nm.

To improve the crystalline perfection and stoichiometry the CeO_2 layers prepared by our deposition techniques (sputtering, evaporation) were annealed ex-situ for 3 hours at 1000°C in the air.

3   Film characterization

In spite of different deposition techniques, there is a number of typical parameters which characterize the prepared CeO_2 films of high quality after post-deposition annealing on R-plane sapphire substrate.

Characteristic features are: smooth surface with average roughness below 0.5 nm for the 1×1 μm^2, only (00l) diffraction lines of the CeO_2, full width at half maximum (FWHM) of the rocking curve of the (002) reflection 0.2-0.4. However, the structural quality is often described using rocking curves, which exhibit two-component shapes, especially for very thin CeO_2 layers.
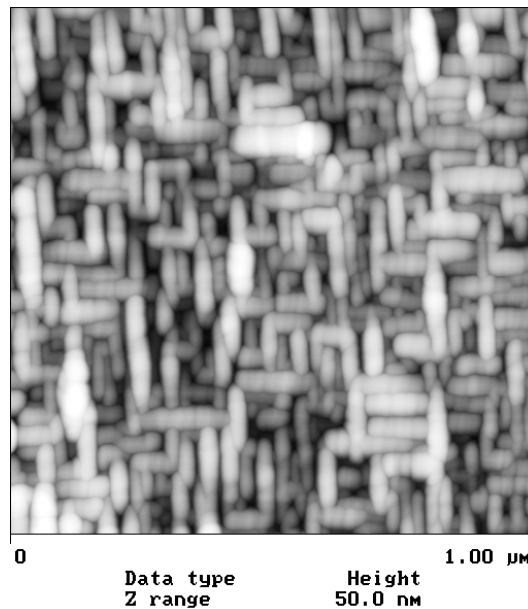
Fig. 1. AFM image of the as-deposited CeO$_2$ film (without (111) peak in X-ray spectrum) on the sapphire substrate.

The rocking curves consist of a broad peak and a narrow one sitting on the top. The best FWHM value for the narrow peak has been recently achieved 0.013° [6]. The origin of such behaviour is discussed by various groups in connection with the effect of structural perfection of the CeO$_2$ films. Especially, the localization of the near perfect CeO$_2$ and the less oriented fraction is still an open question. Buffer layers of only 20 nm thickness inhibit interdiffusion between YBCO and Al$_2$O$_3$.

4   Some experimental results and discussion

In case of electron beam evaporation method, the FWHM value of the rocking curve of highly oriented (001) CeO$_2$ films is $\approx$ 0.4-0.7°. Atomic Force Microscopy (AFM) and X-ray measurements reveal that the presence of even negligible (111) parasitic peak, in X-ray diffraction spectrum of the as-deposited films, strongly correlates with the FWHM of the rocking curve and surface morphology after post-deposition heat treatment in the air. The post-annealing suppress (111) peak in X-ray spectrum, however, the rocking curve becomes very broad (FWHM $\approx$ 2-3°) due to the misorientation of the CeO$_2$ grains in a-b plane. In case of the as-deposited CeO$_2$ film without (111) peak in X-ray spectrum the post-treatment improves the FWHM value of the rocking curves and the surface morphology shows the presence of mosaic blocks (Fig. 1) of dimensions $\approx 100 \times 20$ nm^2 and after post-annealing process the final film has very smooth surface with overlapped blocks (Fig. 2).

In case of the as-deposited - sputtered CeO$_2$ films we observe only granular, columnar character of the films [9, 10] and the post-treatment improves the FWHM of the rocking curves, only.
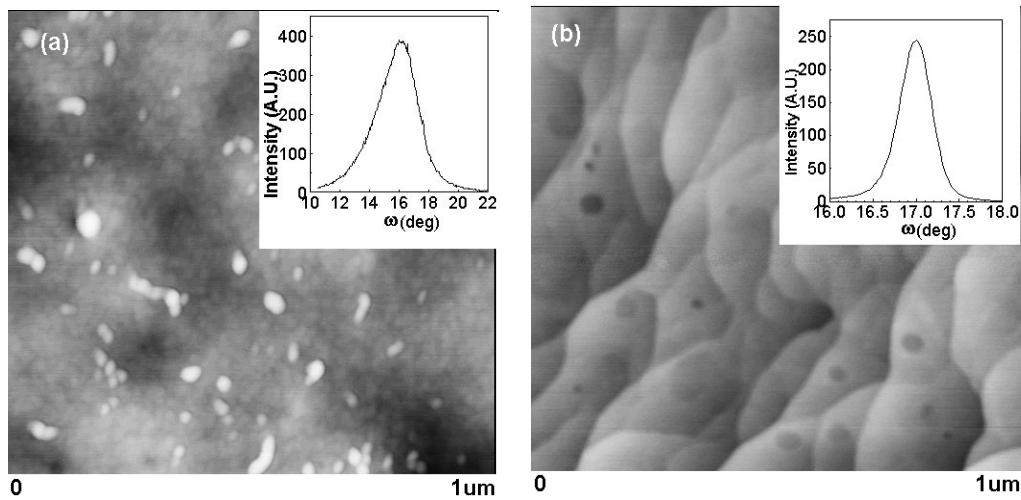
Fig. 2. AFM images of the CeO$_2$ films after post-deposition annealing (a) in case of the presence of (111) peak (b) without (111) peak in X-ray spectrum of the as-deposited films. The insets show the rocking curves of the annealed films.
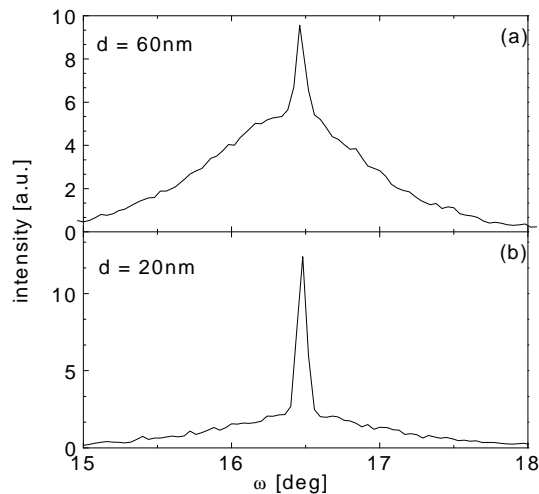

Fig. 3. Rocking curves from the (002) peak of the CeO$_2$ layer deposited by off-axis rf sputtering (T_S = 800°C, p(O$_2$)=8 Pa) with thickness (a) d=60 nm and (b) d=20 nm.

The FWHM values of the as-deposited films reached systematically $< 1°$, while the best values FWHM $\approx 0.2 - 0.4°$ after the post-annealing were achieved. The rocking curve of thinner films (15-60 nm) often shows a superposition of a very sharp peak with FWHM $\approx 0.05 - 0.08°$ and a broad one $\approx 0.4 - 1°$. We found out the shape dependence of the rocking curve on the film thickness [9] (Fig. 3). However, two-component shape of the rocking curve can be influenced by the quality and processing of the sapphire substrate itself [10]. Fig. 4 reveals a clear difference

| non annealed sample | $1 \times 1 \mu m^2$ | annealed sample |

peak-to-valley roughness = 1.85 nm

rms roughness = 0.13 nm

average roughness = 0.1 nm

peak-to-valley roughness = 10.8 nm

rms roughness = 0.87 nm
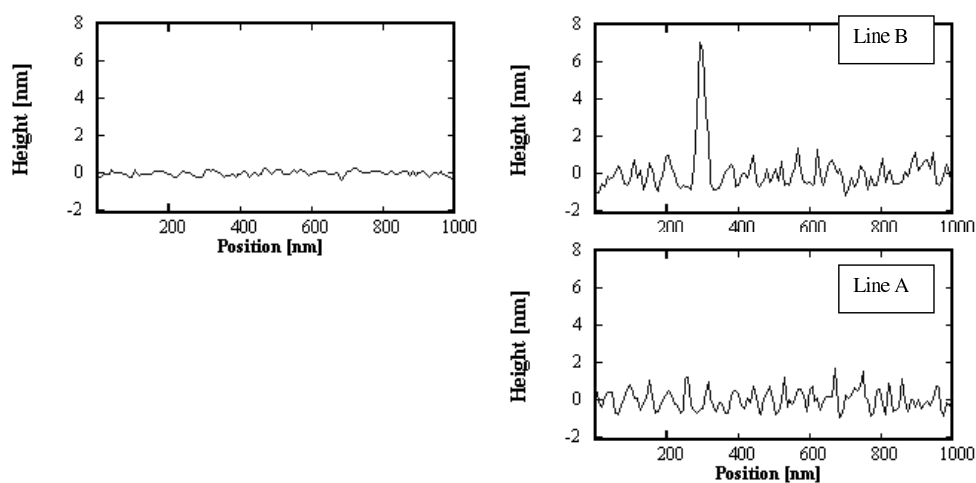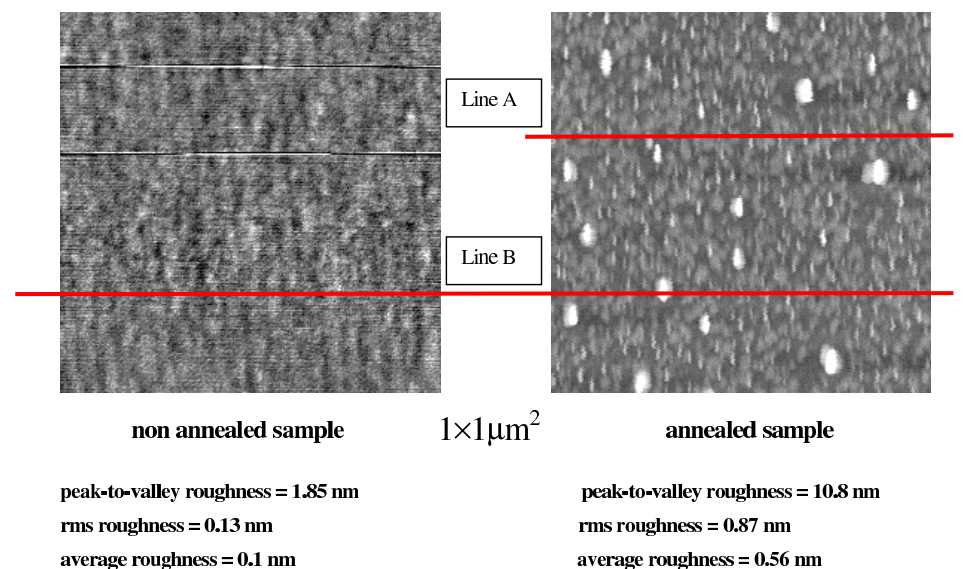
average roughness = 0.56 nm

Fig. 4. AFM comparison between pre-annealed and a non-annealed type sapphire substrate.

between the surface topography of the pre-annealed (3 hours at 1000°C in the air) and the non pre-annealed sapphire substrate. Pre-annealed substrate exhibits an increased roughness and we detect the presence of the outgrowths with a height of 6 nm. Pre-annealed substrate generates reproducibly two-component shape of the rocking curve of the sputtered CeO_2 films. The roughness of these CeO_2 films increased in comparison to the films with prevailingly simple rocking curves prepared on the top of non-annealed substrates.
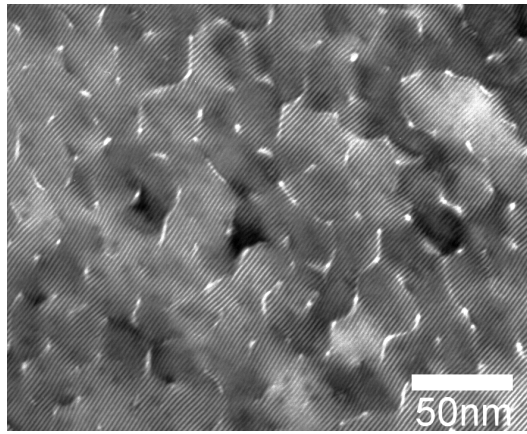
Fig. 5. TEM micrograph of the epitaxial CeO_2 layer deposited on sapphire. The layer consists of misoriented mosaic blocks ($\approx$ 20 nm) separated by voids in some cases.
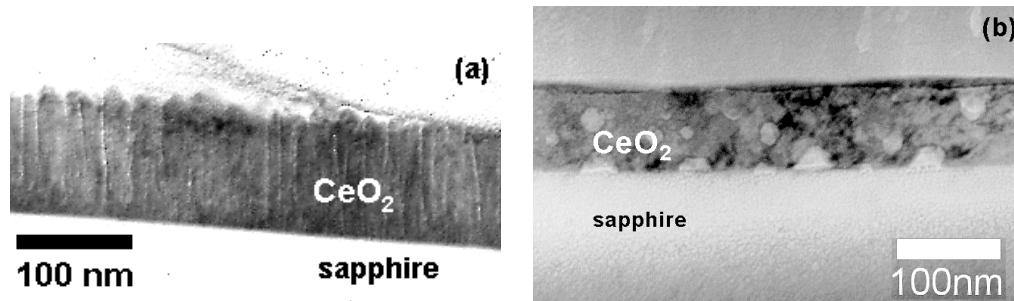

Fig. 6. (a) Cross sectional TEM micrograph of the as-deposited CeO_2/Al_2O_3 with faceted surface structure. Column boundaries form during the initial stage of growth. (b) Cross-sectional TEM micrograph of the annealed CeO_2/Al_2O_3. Due to the recrystallization the boundaries disappears.

The CeO_2 layers with thickness ranging from 15-100 nm exibit the same microstructure. The TEM analysis [9] showed that (001) oriented as-deposited CeO_2 layer consists of a small mosaic blocks with a size of about 20 nm separated by rectangular boundaries (Fig. 5). The cross-sectional TEM micrograph shows a typical columnar structure of the as-deposited epitaxially grown CeO_2 (Fig. 6a). Upon annealing the layer (3 hours at $1000°C$ in the air) the recrystallization of the layer occurs. Beside a decrease of the CeO_2 grain in-plane misorientation (4-$5°$) [9], the adjacent grains are connected creating larger crystallites ($\approx$ 50 nm) (Fig. 6b). We observe the existence of voids with maximum diameter $\approx$ 30 nm distributed through the whole thickness of the CeO_2 films.

Above presented results, the influence of the film thickness and especially the substrate, suggest the origin of near perfect CeO_2 is linked with the surface of the substrate in the form of columns and suppose simultaneous growth of the near perfect material from the beginning of the deposition.

5   Conclusions

High-quality (00l) CeO$_2$ epitaxial films were grown on R-plane sapphire substrate. We have demonstrated that the surface morphology and FWHM values of the rocking curves of the as-deposited films after ex-situ annealing (for 3 hours at 1000°C in the air) are influenced by the type of the deposition technique. We found out the shape dependence of the rocking curve on the film thickness, upon origin and processing of the substrate. This supports the idea that the near perfect CeO$_2$ has the origin at the substrate. As-deposited CeO$_2$ layers consist of a small mosaic blocks, with a size of about 20 nm and separated by boundaries, which increase to a size ≈ 50 nm (simultaneously with the existence of voids) after ex-situ annealing.

References

[1] F. Wang, R. Wordenweber: *Thin Solid Films* **227** (1993) 200

[2] Yu.A. Boikov, T. Claeson, D. Erts, F. Bridges, Z. Kvitky: *Phys. Rev. B* **56** (1997) 11312

[3] W.L. Holstein, L. A. Parisi, D. W. Face: *Appl. Phys. Lett.* **61** (1992) 982

[4] M. Maul, B. Schulte, P. Haussler, G. Frank, T. Steinborn, H. Fuess, H. Adrian: *J. Appl. Phys.* **74** (1993) 2942

[5] C. Tian, Y. Du, S.-W. Chan: *J. Vac. Sci. Technol. A* **15** (1997) 85

[6] A. G. Zaitsev, G. Ockenfuss, D. Guggi, R. Wordenweber: *J. Appl. Phys.* **81** (1997) 3069

[7] C.C. Chin, R.J. Lin, Y.C. Yu, C.W. Wang, E.K. Lin, W.C. Tsai, T.Y. Tseng: *Physica C* **260** (1996) 86

[8] X. Castel, M. Guilloux-Viry, A. Perrin, J. Lesueur, F. Lalu: *Journal of Crystal Growth* **187** (1998) 211

[9] M. Španková, I. Vávra, Š. Gaži, D. Machajdík, Š. Chromik, K. Fröhlich, L. Hellemans, Š. Beňačka: *Journal of Crystal Growth*, to appear

[10] Š. Chromik *et al.*: submitted

[11] R. Körner, M. Ricken, J. Nölting, I. Reiss: *J. Solid State Chem.* **78** (1989) 136